Magazine of Civil Engineering

ISSN 2071-0305

journal homepage: http://engstroy.spbstu.ru/

DOI: 10.18720/MCE.95.4

Destruction of powder-activated concrete with fixation of destruction by a laser interferometer

V.I. Travush[a], N.I. Karpenko[a], V.T. Erofeev[b*], N. Vatin[c], I.V. Erofeeva[b], I.N. Maksimova[d], V.I. Kondrashchenko[e], A.G. Kesarijskij[f]

[a] *Russian Academy of Architecture and Building Sciences, Moscow, Russia*

[b] *Ogarev Mordovia State University, Saransk, Russia*

[c] *RUDN University, Moscow, Russia*

[d] *Penza State University of Architecture and Construction, Penza, Russia*

[e] *Russian University of Transport, Moscow, Russia*

[f] *LLC "Laboratory of integrated technology", Pavlograd, Ukraine*

** E-mail: yerofeevvt@mail.ru*

Keywords: self-compacting concrete, fracture testing, sress-strain curves, crack propagation, laser interferometry

Abstract. The article is devoted to the identification of the patterns of deformation and destruction of powder-activated concrete under the action of power loads. As research concrete, powder-activated concrete of a new generation was considered in comparison with materials of the old and transitional generations. To carry out such studies, laser holographic interferometry methods were used, the physical essence of which consists in recording wave fields synchronously with the application of the load reflected by the surface under study at various points in time and then comparing these wave fields with each other. Using the complete equilibrium deformation diagrams and 3D graphs, we determined the parameters of the diagram (cyclicity, ultimate tensile strength), and the parameters of surface deformation (photographs with waves of strains and cracks). Using laser interferometry methods, it was found that the introduction of microquartz, especially in combination with amorphous active silica fume, significantly delays the onset of microcrack formation in cement samples, which exhibit a uniform deformation field up to a stress level of 0.90–0.95 from destructive. A sample based on a cement-sand mortar without finely dispersed fillers distinguishes a lower level of crack formation, corresponding to a stress level of 0.5–0.6 from destructive ones, and with an increase in load, the fracture of the sample has a block character.

1. Introduction

The composition of concrete in various proportions includes aggregates, a binder, water and modifying additives (plasticizing, reactive microbiological, etc.), included depending on the required strength and its functional purpose [1–8]. High-quality concretes (HQC) classification combine a wide range of concretes for various purposes: high-strength (HSB, HochfesterBeton – HFB) and ultrahigh-strength (UVB, UltrahochfesterBeton – UHFB), self-compacting (SUB, Selbstverdichtender Concrete); joint-stock powder, dispersion-reinforced (ReaktionspulverBeton – RPB or ReactivePowderConcrete – RPC) and others. These types of concrete satisfy the high requirements for compressive and tensile strength, crack resistance, impact strength, wear resistance, corrosion resistance, frost resistance and other key performance indicators [2, 6, 9–12].

Travush, V.I., Karpenko, N.I., Erofeev, V.T., Vatin, N., Erofeeva, I.V., Maksimova, I.N., Kondrashchenko, V.I., Kesarijskij, A.G. Destruction of powder-activated concrete with fixation of destruction by a laser interferometer. Magazine of Civil Engineering. 2020. 95(3). Pp. 42–48. DOI: 10.18720/MCE.95.4

The development of concrete science is connected with the concept of highly functional concretes (High Performance Concrete – LDC). One of its developers, the Canadian scientist P.-K. Aichin notes its difference from the concept of high-strength concrete (High Strength Concrete (HSC). P.-K. Aichin and his followers [13, 14] saw the development of high-functional concrete technology [13, 14] when they achieved the highest possible strength indicators (R_s = 140 MPa), manufacturability, density and durability. The use of high-strength concrete is the most effective way to reduce the mass of structures, the complexity and cost of their construction, which necessitates the creation of new types of them with increased strength and durability. Important in this case is the physicochemical dispersion of highly concentrated mineral powders of various chemical and mineralogical nature for the production of building materials with extremely long aggregate stability.

Experimental evidence of the achievement of water-reducing effects equal to 8–15 versus 1.8–2.0 in cement dispersions is given in [5]. In these experiments, the gravitational fluidity of plasticized mineral suspensions was maintained while reducing water consumption by 8–15 times! It is such cardinal changes in the rheological properties and water-reducing effects that served as the basis for the creation of high-strength and ultra-high-strength concrete of the new generation [5, 14–16]. A new progress strategy was formulated in obtaining highly filled and highly economical concrete of ordinary grades M200–M600 and high-strength concrete M600–M1000, high-strength and ultra-high-strength: “Through a rational rheology into the future of concrete” [14, 15]. For enhanced implementation of the construction of new varieties of concrete in practice, it is necessary to take into account all their advantages in comparison with traditional materials. For the successful implementation of the construction of new varieties of concrete in practice, it is necessary to take into account all their advantages in comparison with traditional materials, in connection with which an important direction is to conduct research on materials to optimize them in terms of static and dynamic strength, durability. At the same time, along with the establishment of physic-mechanical parameters of cement composites, it is necessary to identify the patterns of their deformation and fracture under the action of power loads [17–21].

Traditional methods for studying the mechanics of concrete fracture involves loading the test sample and recording its deformation response depending on the magnitude of the load. This approach is quite simple and convenient, but gives information only about the limiting states of the object. At the same time, for specialists in the field of mechanics of a deformed solid and the calculation of building structures, an important role is played by an understanding of the process of destruction of a material and its behavior at all stages of testing.

The objects of research were powder-activated concretes with a high proportion of the suspension component, which included, along with cement, sand and water, superplasticizer, rheologically active and reactive additives. Concrete of transitional and old generations were considered as compared materials. Old-generation concretes were formed from a cement-sand mixture, with a superplasticizer, of a transitional type – with the addition of a reactive active additive – silica fume.

The goal of our work was to study the stages of development of the processes accompanying the destruction of samples, with the fixation of the fields of deformation movements synchronously with the application of the load.

The objectives of the research were:

1. Investigate the stage of destruction of samples of powder-activated concrete;
2. To compare the performance of powder-activated concrete with concrete of the old and transitional generations;
3. To identify the effect of water-cement ratio, the content of superplasticizer, finely dispersed fillers on crack formation.

2. Methods

The tests were performed using laser holographic interferometry methods, the promisingness of which for the study of building materials of complex structures was confirmed by a number of successful experimental studies that revealed previously unknown features of the fracture mechanics of various building materials, including those based on cement binders [22–27].

Cement composites were made on CEM I 42.5 N cement of the Ulyanovsk cement plant of the Russian Federation: cement composite with Melflux 1641F hyperplasticizer filled with sand of fractions 0–0.63 and 0.63–2.5 mm (composition No. 6); cement composite with Melflux 1641F hyperplasticizer, filled with sand fractions 0–0.63 and 0.63–2.5 mm with the addition of microquartz (composition No. 4); cement composite with Melflux 1641F hyperplasticizer filled with sand of fractions 0–0.63 and 0.63–2.5 mm with the addition of microquartz and silica fume (composition No. 5).

To load the samples, a press with a force of up to 200 kN equipped with a power hydraulic cylinder was used.

The analysis of interferograms was performed according to the method described in [8, 22], where the displacement at a point was determined by the formula:

$$\vec{d}(\vec{r}_i + \vec{r}_o) = \lambda n, \quad (1)$$

where $\vec{d}$ is the vector of displacement of a point on the investigated surface;

$\vec{r}_i$ is a single vector of illumination of the investigated surface;

$\vec{r}_o$ is a single observation vector of the investigated surface;

λ is wavelength of laser radiation;

n is the order of the interference band.

The experimental data were processed using the AutoCAD graphic complex. In Fig. 1 shows one of the interferograms at the stage of decryption.

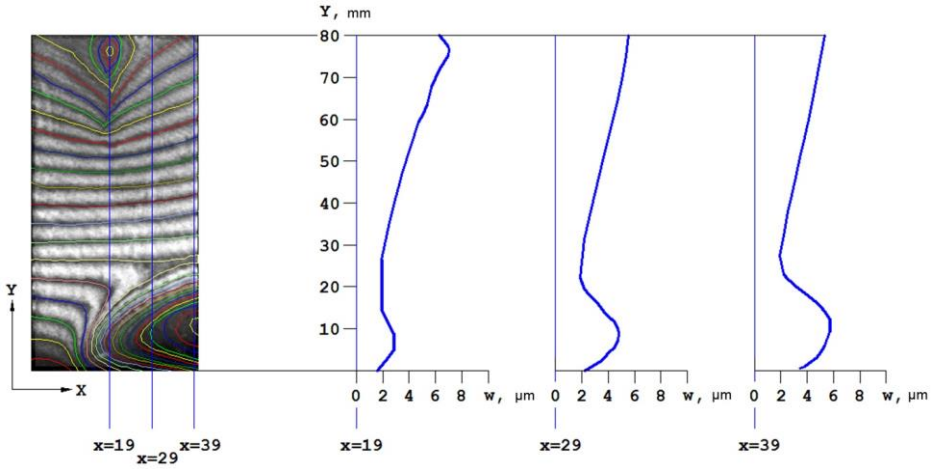

Figure 1. Interpretation of the interferogram with the construction of graphs of the field of movement along the sections.

For a more visual representation of the deformation of the sample, 3D visualization of the displacement field, shown in Fig. 2, which significantly reduces the analysis time of interferograms.

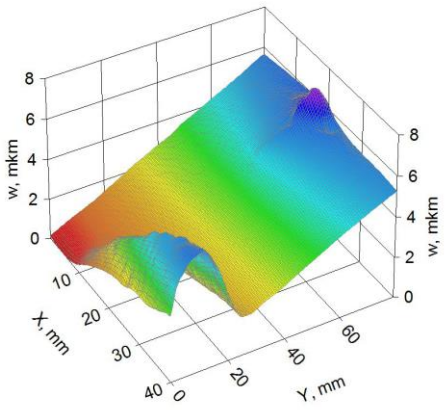

Figure 2. Presentation of data on the field of movement of the sample in the form of 3D graphics.

The effect of microquartz (composition No. 4) or a mixture of microquartz with silica fume (composition No. 5) on the properties of sand concrete was studied by comparison with a control composition that does not contain finely dispersed quartz (composition No. 6). In all the studied compositions, in addition to cement and water, Melflux 1641F brand hyperplasticizer and two-fraction quartz sand were used. To ensure equal mobility of the cement-sand mortar, the water-cement ratio of the control composition was 14 % lower than that of the composition on microquartz, and 9.5 % lower than that of the composition on a mixture of microquartz and silica fume. The latter is explained by the plasticizing effect of microquartz.

3. Results and Discussion

Interferograms, 3D-graphs, surface deformations and deformations for samples of compositions 6, 4 and 5 are shown in Figs. 3, 4 and 5.

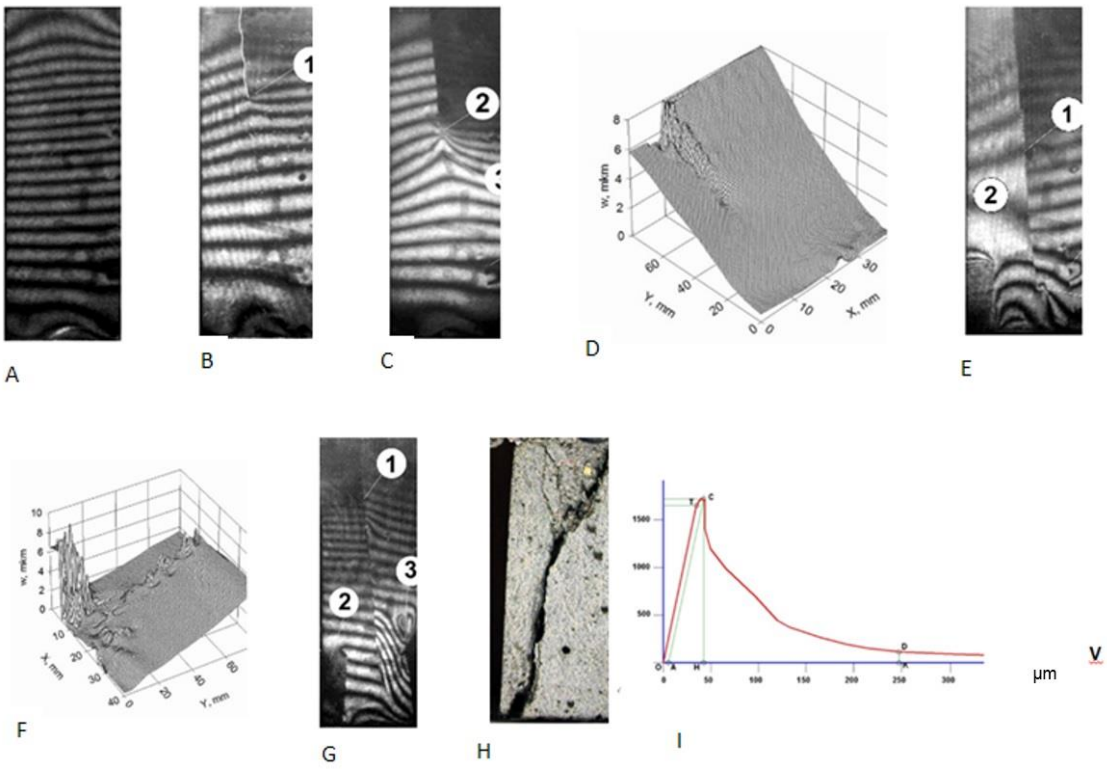

Figure 3. Interferograms (A–C, E, G), 3D-graphs (D, F) of surface deformations and a photograph (H) complete equilibrium deformation diagram (I) of sample No. 6 ($\Delta\sigma$ = 1.53 MPa, other explanations are given in the text).

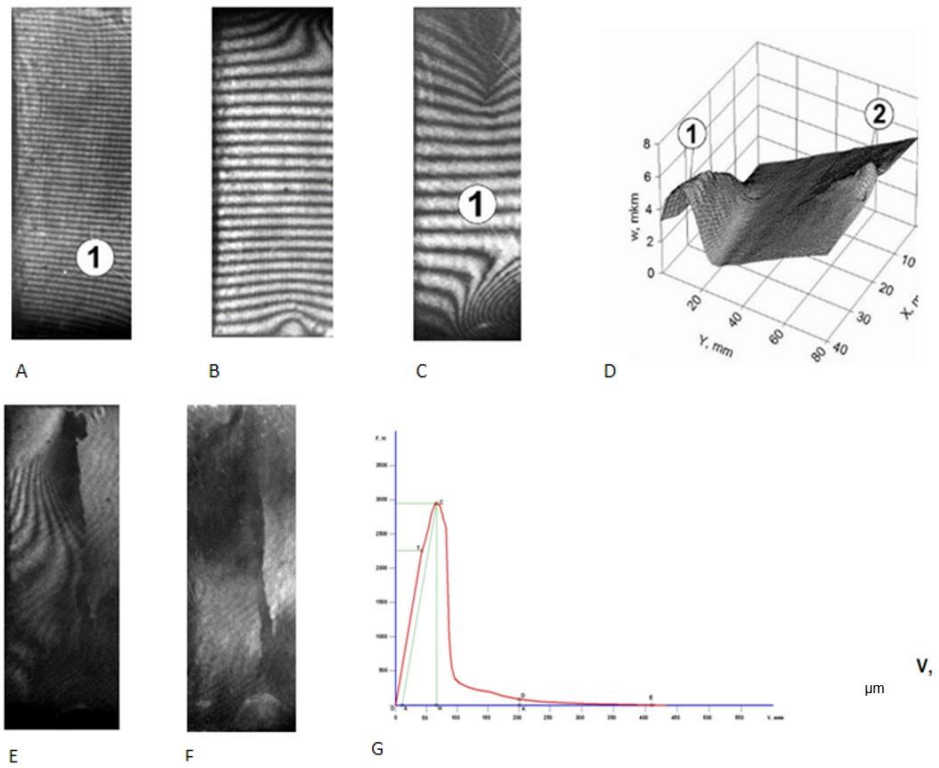

Figure 4. Interferograms (A–C, E, F) and 3D-graph (D) of surface deformations, complete equilibrium deformation diagram (G) of specimen composition No. 4 ($\Delta\sigma$ = 1.53 MPa, other explanations are given in the text).

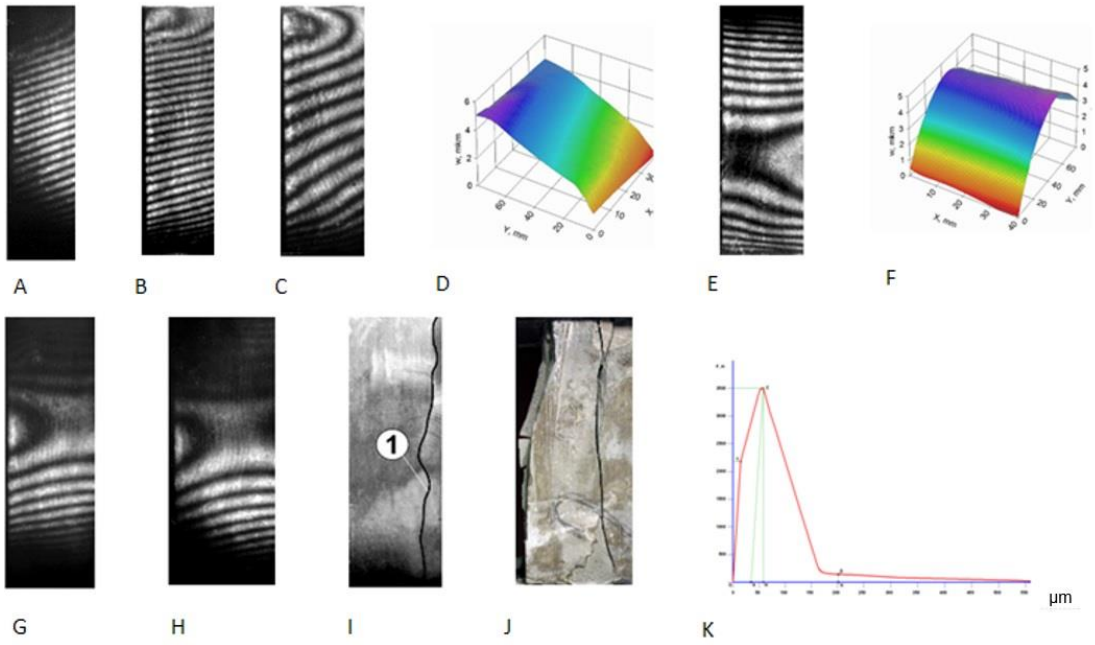

Figure 5. Interferograms (A–C, E, G–I), 3D-graphs (D, F) of surface deformations and a photograph (K) complete equilibrium deformation diagram (I) of sample No. 5 ($\Delta\sigma$ = 1.53 MPa, others explanations are given in the text).

In concrete without quartz micro-filler (composition No. 6) at a stress level of 0.27σ size. Deformation of the sample is observed as an isotropic body with minor anomalies in the zone of its contact with the loading plates of the press (Fig. 3). With an increase in load to 0.59σ a zone of increased plastic deformations is identified, identified as a visually unobservable crack, and a slight anomaly appears in the zone of local deformation of the sample, which, with an increase in stresses up to 0.72σ, develops with the formation of new anomalous zones. At a stress level of 0.82σ the vertical zone of plastic deformation almost completely intersects the surface of the sample, dividing it into two blocks, but is inhibited by the structural element of the material. In the lower left part of the sample, a zone of high gradient deformation develops, parallel to the crack, dividing it into two subunits. The previously observed anomaly forms a local crack. The formed blocks behave as separate elastic elements with substantially different deformation fields. At a stress level of 0.95σ the main crack develops along the entire length of the sample.

A fragment in the lower left corner of the sample undergoes continuous movement. The abnormal zone in this case generates a third vertical crack, which provides freedom of movement to the newly formed block. The destruction of the sample is observed, in which large blocks are held by a geometric closure at the boundary of their surfaces before its physical disintegration into fragments by a main crack.

In samples with microquartz at a stress level of 0.15σ_{destr} local microfractures are observed in the zone of their contact with the loading plates, associated with roughnesses in the end surfaces and their hugging with increasing load, which develop with increasing load and manifest themselves at a stress level of ≈ 0.5σ_{destr}, leading to the onset of the formation of a main crack along the compressive load and initially not visually detectable even at a stress level of 0.91σ_{destr}, and then clearly observed on the interferogram at a stress level of ≈ σ_{destr}.

For a sample with microquartz and silica fume with an increase in the load from the stress level 0.13σ_{destr} до 0.26σ_{destr} the field of displacements over the entire surface of the sample remains uniform, without local anomalies.

At a stress level of 0.47σ the local annular structure of interference fringes in the upper left corner of the sample indicates a shift in the contact forces to this zone, which is explained by the ongoing pressure testing of its surfaces in contact with the press plate. For most of the sample, uniform deformation is observed without signs of abnormal plastic deformations. Increment of stresses by 38 % – from level 0.47σ_{destr} до 0.65σ_{destr} caused deformation of the central part of the sample, which is explained by the manifestation of the "cage effect" – its cramped deformations in the zone of contact with the press plates.

At this level of stress, zones of abnormal plastic deformations are still not observed, in contrast to the composition with microquartz, which has a stress level of ≈ 0.5σ_{destr} the beginning of the formation of a main crack, or a control composition, was observed, in which, at a stress level of 0.59σ_{destr}, a zone of increased

plastic deformation appeared, identified as a visually unobservable crack and a zone of local deformation of the sample.

At a voltage level of $0.78\sigma_{destr}$ up to $0.91\sigma_{destr}$ the nature of the displacement field does not change significantly – there are no local anomalies, there are no signs of crack nucleation, which fundamentally distinguishes the behavior of the composition with microquartz and silica fume from other studied compositions. In this case, the loss of contrast of the interference bands in the upper and lower parts of the sample is explained by the beginning of its destruction in the contact zone with the reference and loading plate presses. Such a uniform deformation of the sample up to a load of more than $0.9\sigma_{destr}$ resulted at a stress level of $\approx 1.0\sigma_{destr}$ spontaneous development, apparently, from the zones of contact of the sample with the support and loading plates of the press of a vertically directed main crack, which divided the sample into two equal fragments.

4. Conclusion

1. The relevance of researching the durability of concrete is shown, since structures based on them are subject to cracking during operation. The purpose of the study was to study the stages of development of the processes accompanying the destruction of concrete samples by laser interferometry with fixation of the fields of displacements synchronously with the application of the load.

2. As a result of the research revealed the following:

- A decrease in W / C causes a more elastic behavior of the material under load, a significant (4–5 times) lengthening of the descending branch of the full equilibrium diagram of the deformation of cement stone and a change in the fracture mechanism of the material, with W / C 0.267, through the formation of a main crack in the early stages of loading and its subsequent development up to the fragmentation of the sample, and at W / C 0.350 – through the formation of a block structure with the subsequent closure of transverse cracks in the blocks and the merging of longitudinal block cracks into a main crack;
- Laser interference studies generally confirmed the block nature of the prefracture of the specimen with the Melflux 1641F hyperplasticizer, followed by the formation of a main (main) crack, leading to its physical destruction and fragmentation into separate plates.

Using laser interferometry methods, it was found that the introduction of microquartz, especially in combination with amorphous active silica fume, significantly delays the onset of microcrack formation in cement samples, which exhibit a uniform deformation field up to the stress level of $0.90\sigma_{destr} – 0.95\sigma_{destr}$ Cement-sand stone without finely dispersed quartz distinguishes a lower level of crack formation, corresponding to a stress level of $0.5\sigma_{destr} – 0.6\sigma_{destr}$ from destructive ones, and with an increase in load, the fracture of the sample has a block character.

References

1. Bazhenov, Yu.M., Chernyshev, Ye.M., Korotkikh, D.N. Konstruirovaniye struktur sovremennykh betonov: opredelyayushchiye printsipy i tekhnologicheskiye platform [Structural engineering of modern concrete: defining principles and technological platforms]. Stroitelnyye materialy. 2014. No. 3. Pp. 6–15. (rus)
2. Erofeev, V.T., Rodin, A.I., Yakunin, V.V., Bogatov, A.D., Bochkin, V.S., Chegodajkin, A.M. Alkali-activated slag binders from rock-wool production wastes. Magazine of Civil Engineering. 2018. 82(6). Pp. 219–227. DOI: 10.18720/MCE.82.20
3. Zhao, Q., Cheng, P., Wei, Y., Wang, J. Factors effecting the recovery process of self-repairing concrete. Magazine of Civil Engineering. 2019. 88(4). Pp. 52–59. DOI: 10.18720/MCE.88.5
4. Igawa, H., Eguchi, H., Kitsutaka, Y. A fundamental study for the self-healing performance of heavyweight concrete. Journal of Structural and Construction Engineering. 83(748). Pp. 763–772. DOI: 10.3130/aijs.83.763.
5. Kalashnikov, V.I. Terminologiya nauki o betone novogo pokoleniya [New Generation Concrete Science Terminology]. Stroitelnyye materialy. 2011. No. 3. Pp. 103–106. (rus)
6. Kapriyelov, S.S., Chilin, I.A. Sverkhvysokoprochnyy samouplotnyayushchiysya fibrobeton dlya monolitnykh konstruktsiy [Ultra-high-self-sealing fiber concrete for monolithic constructions]. Beton i zhelezobeton – vzglyad v budushcheye : nauchnyye trudy III Vserossiyskoy (II Mezhdunarodnoy) konferentsii po betonu i zhelezobetonu: v 7 t. T. 3 [Concrete and reinforced concrete – a look into the future: scientific papers of the III All-Russian (II International) conference on concrete and reinforced concrete: in 7 vol. V. 3]. Moscow : MGSU, 2014. Pp. 158–164. (rus)
7. Makar, J., Margeson, J., Luh, J. Carbon nanotube/cement composites – early results and potential applications. 3-id International Conference on Construction Materials: Performance, Innovations and Structural Implications. Vancouver, B.C. 2005. Pp.1–10.
8. Cwirzen, A., Habermehl-Cwirzen, K., Penttala, V. Surface decoration of carbon nanotubes and mechanical properties of cement/carbon nanotube composites. Advances in Cement Research. 2008. 20(2). Pp. 65–73. DOI: 10.1680/adcr.2008.20.2.65
9. Kalinovskiy, M.I. Primeneniye fibry dlya povysheniya treshchinostoykosti betona [The use of fiber to increase the crack resistance of concrete]. Transportnoye stroitelstvo. 2008. No. 3. Pp. 7–9. (rus)
10. Akimov, L., Ilenko, N., Mizharev, R., Cherkashin, A., Vatin, N., Chumadova, L. Influence of Plasticizing and Siliceous Additives on the Strength Characteristics of Concrete. Applied Mechanics and Materials. 2015. No. 725–726. Pp. 461–468. DOI: 10.4028/www.scientific.net/AMM.725-726.461

11. Beygi, M.H.A., Kazemi, M.T., Nikbin, I.M., Amiri, J.V. The effect of water to cement ratio on fracture parameters and brittleness of self-compacting concrete. Materials and Design. 2013. No. 50. Pp. 267–276. DOI: 10.1016/j.matdes.2013.02.018
12. Carpinteri, A., Brighenti, R. Fracture behaviour of plain and fiber-reinforced concrete with different water content under mixed mode loading. Materials and Design. 2010. 31(4). Pp. 2032–2042. DOI: 10.1016/j.matdes.2009.10.021
13. Aitcin, P.-C., Neville, A. High Performance Concrete Demystified. Concrete International. 1993. 15(1). Pp. 21–26.
14. Kalashnikov, V., Kornienko, P., Gorshkova, L., Gakshteter, G., Sarsenbayeva, A. Development of compositions of self-compacting fine-grained refractory concrete. Journal of Advanced Concrete Technology. 2014. 12(9). Pp. 299–309. DOI: 10.3151/jact.12.299
15. Yerofeyeva, I.V. Fiziko-mekhanicheskiye svoystva, biologicheskaya i klimaticheskaya stoykost poroshkovo-aktivirovannykh betonov: avtoreferat dissertatsii kand. tekhn. nauk [Physico-mechanical properties, biological and climatic resistance of powder-activated concrete: abstract of the thesis of Cand. tech. sciences]. Penza, 2018. 28 p. (rus)
16. Zhang, X.X., Ruiz, G., Yu, R.C., Tarifa, M. Fracture behaviour of high-strength concrete at a wide range of loading rates. International Journal of Impact Engineering. 2009. 36(10-11). Pp. 1204–1209. DOI: 10.1016/j.ijimpeng.2009.04.007
17. Sprince, A., Pakrastinsh, L., Vatin, N. Crack Formation in Cement-Based Composites. IOP Conference Series: Materials Science and Engineering. 2016. 123(1). 012050. DOI: 10.1088/1757-899X/123/1/012050
18. Muralidhara, S., Prasad, B.K.R., Eskandari, H., Karihaloo, B.L. Fracture process zone size and true fracture energy of concrete using acoustic emission. Construction and Building Materials. 2010. 24(4). Pp. 479–486. DOI: 10.1016/j.conbuildmat.2009.10.014
19. Shah, S.G., Kishen, J.M.C. Fracture Properties of Concrete-Concrete Interfaces Using Digital Image Correlation. Experimental Mechanics. 2011. 51(3). Pp. 303–313. DOI: 10.1007/s11340-010-9358-y
20. Zhang, X.X., Yu, R.C., Ruiz, G., Tarifa, M., Camara, M.A. Effect of loading rate on crack velocities in HSC. International Journal of Impact Engineering. 2010. 37(4). Pp. 359–370. DOI: 10.1016/j.ijimpeng.2009.10.002
21. Dong, W., Zhou, X., Wu, Z. On fracture process zone and crack extension resistance of concrete based on initial fracture toughness. Construction and Building Materials. 2013. No. 49. Pp. 352–363. DOI: 10.1016/j.conbuildmat.2013.08.041
22. Vest, Ch. Gologaficheskaya interferometriya [Holographic interferometry]. Moscow: Mir, 1982. 504 p. (rus)
23. Chernyshov, Ye.M., Korotkikh, D.N. Modifitsirovaniye struktury tsementnogo kamnya mikro- i nanorazmernymi chastitsami kremnezema (voprosy teorii i prilozheniy) [Modification of the structure of a cement stone by micro- and nanosized particles of silica (theory and application issues)]. Stroitelnyye materialy, oborudovaniye i tekhnologii XXI veka. 2008. No. 5. Pp. 30–32. (rus)
24. Matallah, M., La Borderie, C., Maurel, O. A practical method to estimate crack openings in concrete structures. International Journal for Numerical and Analytical Methods in Geomechanics. 2010. 34(15). Pp. 1615–1633. DOI: 10.1002/nag.876
25. Alam, S.Y., Saliba, J., Loukili, A. Fracture examination in concrete through combined digital image correlation and acoustic emission techniques. Construction and Building Materials. 2014. No. 69. Pp. 232–242. DOI: 10.1016/j.conbuildmat.2014.07.044
26. Skarzyński, Ł., Kozicki, J., Tejchman, J. Application of DIC Technique to Concrete-Study on Objectivity of Measured Surface Displacements. Experimental Mechanics. 2013. 53(9). Pp. 1545–1559. DOI: 10.1007/s11340-013-9781-y
27. Alam, S.Y., Loukili, A., Grondin, F. Monitoring size effect on crack opening in concrete by digital image correlation. European Journal of Environmental and Civil Engineering. 2012. 16(7). Pp. 818–836. DOI: 10.1080/19648189.2012.672211

Contacts:

Vladimir Travush, travush@mail.ru
Nikolaj Karpenko, karpenko@raasn.ru
Vladimir Erofeev, yerofeevvt@mail.ru
Nikolai Vatin, vatin@mail.ru
Irina Erofeeva, ira.erofeeva.90@mail.ru
Irina Maksimova, maksimovain@mail.ru
Valerij Kondrashchenko, kondrashchenko@mail.ru
Aleksandr Kesarijskij, algeo57k@gmail.com